Failure analysis of uncooled infrared focal plane array under a high-*g* inertial load

2006 Meas. Sci. Technol. 17 2969

(http://iopscience.iop.org/0957-0233/17/11/016)

INSTITUTE OF PHYSICS PUBLISHING MEASUREMENT SCIENCE AND TECHNOLOGY

Meas. Sci. Technol. **17** (2006) 2969–2972 doi:10.1088/0957-0233/17/11/016

Failure analysis of uncooled infrared focal plane array under a high-*g* inertial load

Shali Shi[1], Dapeng Chen[1], Chaobo Li[1], Binbin Jiao[1], Yi Ou[1], Yupeng Jing[1], Tianchun Ye[1], Zheying Guo[2], Qingchuan Zhang[2] and Xiaoping Wu[2]

[1] Institute of Microelectronics of Chinese Academy of Sciences, Beijing 100029, People's Republic of China
[2] University of Science and Technology of China, Hefei, People's Republic of China

E-mail: dpchen@ime.ac.cn

Received 11 May 2006, in final form 24 July 2006
Published 5 October 2006
Online at stacks.iop.org/MST/17/2969

Abstract

This paper describes the failure analysis of an uncooled infrared focal plane array (IRFPA) under a high-*g* inertial load system using finite element simulation and experimental validation methods. The uncooled IRFPA, responding to a source of infrared (IR) radiation with spectral range from 8 μm to 14 μm, is a cantilever array, which consists of two materials with mismatched thermal expansion coefficients. The radiance distribution of the IR source could be obtained by measuring the thermal–mechanical rotation angle distribution of every pixel in the cantilever array using a visible optical readout method. Based on this principle, room-temperature infrared imaging was developed under a static gravity environment, as described in our previous paper (Li C *et al* 2006 *Meas. Sci. Technol.* **17** 1981–6). But under a dynamic inertial load, the rotation angle of every pixel includes not only the thermal–mechanical part but also a part induced by the inertial load. In the elastic deformation range, with a linearly increasing acceleration, the deformation angle induced by the inertial load increases linearly, which is validated by finite element simulation. This linear change in deformation, which can be subtracted from the total rotation angle in the optical readout using certain arithmetic, will not influence the imaging result. It is noteworthy that failure stress will occur when the deformation angle induced by the inertial load moves into the plastic deformation range, and the optical readout cannot image the IR object. Through finite element simulation the critical load resulting in IRFPA failure is 2715*g*, and this can be validated through impact using a Hopkinson bar after the IRFPA is placed in vacuum. By finite element simulation, the initial IRFPA surface profile without IR radiance after the 2715*g* load showed a conicoid characteristic. Simulation of the failure analysis of the uncooled IRFPA under 2715*g* acceleration predicts the military application of IRFPAs for an uncooled infrared imaging system in the high-*g* tactical range.

Keywords: failure analysis, high-*g*, elastic deformation, plastic deformation, FPA, IR, optical readout, finite element

(Some figures in this article are in colour only in the electronic version)

1. Introduction

Uncooled infrared imaging systems are widely used in military and civil applications with a high-g tactical range [2–5], yet the failure analysis of overloading upon an IRFPA has seldom been presented. This paper describes the failure analysis of an uncooled IRFPA under a high-g inertial load system using finite element simulation and experimental validation methods. The extreme overloading analysed suggests a limit of application of an uncooled optomechanical IR imaging system in the high-g tactical range.

2. Principles and simulations

The IRFPA is the main part in the uncooled optomechanical IR imaging system (figure 1), which consists of three parts: an IR lens, the IRFPA and the optical readout [6]. The principle of an IR imaging system based on the optomechanical effect is that the bi-material cantilevers—one is Au, the other is SiN_x—bend after absorbing infrared radiation; simultaneously an optical readout measures the deformation of every cantilever of the IRFPA and projects a visible imaging result.

Figure 2 shows the dimensions of each pixel in the IRFPA. The maximum thermal–mechanical rotation angle induced by IR radiation of the object can be read out by the optomechanical readout system (see figure 1). It can be expressed as follows [7]:

$$S_T = \frac{\Delta\theta_{\max}}{\Delta T_s} = \frac{\Delta\theta_{\max}}{\Delta T_c}\frac{\Delta T_c}{\Delta T_s} = \left[9(\alpha_1-\alpha_2)\left(\frac{n+1}{h_2 K}\right) l_{\mathrm{SiN_x,Au}}\right] \times \left[\frac{1}{G_{\mathrm{Total}}}\frac{A_{\mathrm{ab}}\tau\varepsilon\pi}{4F_{\mathrm{no}}^2}\frac{\mathrm{d}L}{\mathrm{d}T_s}\right] \quad (1)$$

where $(\alpha_1 - \alpha_2)$ is the difference in thermal expansion coefficient of Au and SiN_x, K is the structure parameter given by

$$K = 4 + 6n + 4n^2 + \phi n^3 + \frac{1}{\phi n},$$

n is the thickness ratio of Au film and SiN_x film ($n = h_1/h_2$), ϕ is the Young's modulus ratio of Au and SiN_x ($\phi = E_1/E_2$), $l_{\mathrm{SiN_x,Au}}$ is the length of each bi-material supporting beam. G_{Total} is the total thermal conductance of the cantilever structure; A_{ab} is the pixel IR absorption area; τ (= 0.4) is the transmissivity of the IR optical system; ε is the total emissivity due to a distant blackbody source (to a human being ε = 0.98 at a temperature of 300 K); F_{no} (= 0.7) is the F number of the IR imaging lens; the numerical value of $\mathrm{d}L/\mathrm{d}T_s$ in the wavelength range 8–14 μm for a blackbody at a temperature of 300 K is 0.63 W m^{-2} K^{-1} sr^{-1}.

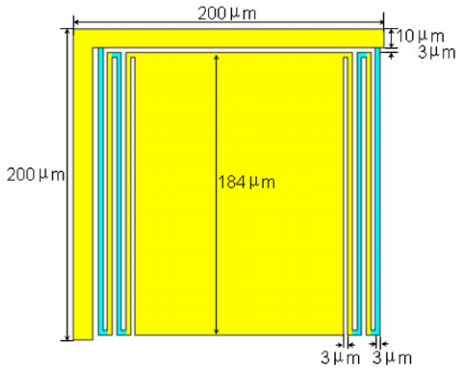

Figure 2. Dimensions of pixels in the IRFPA.

The optomechanical readout system transforms the maximum thermal–mechanical rotation angle of every pixel into a corresponding grey distribution for the thermal image, which obeys the following law:

$$\frac{\Delta I}{\Delta T_S} = \frac{\Delta I}{\Delta\theta}\frac{\Delta\theta}{\Delta T_s} = \frac{\Delta I_{\max}}{\Delta\theta_{\max}}\frac{\Delta\theta_{\max}}{\Delta T_s} = \gamma S_T \quad (2)$$

where $\gamma = \frac{\Delta I}{\Delta\theta}$ is the optical detection sensitivity. Equation (2) is valid when ΔI varies linearly with changing $\Delta\theta$.

Equations (1) and (2) are the imaging principles of IRFPA in the static state. When it is placed in a dynamic inertial load environment, the rotation angle of each pixel includes not only the thermal–mechanical deflection but also the acceleration-induced deformation. The latter should be subtracted by the optomechanical readout system, in order to reflect the exact IR imaging. According to the elastic theory, in the elastic deformation field, with the acceleration increasing linearly, the deformation angle induced by the inertial load increases linearly, and the additional grey change in the thermal image is linear. This could be subtracted during image processing. This elastic theory is validated by finite element simulation as shown in figure 3.

As the inertial load acceleration increases, the stress within each pixel in the IRFPA increases. According to the result of the finite element simulation (figures 4 and 5), when

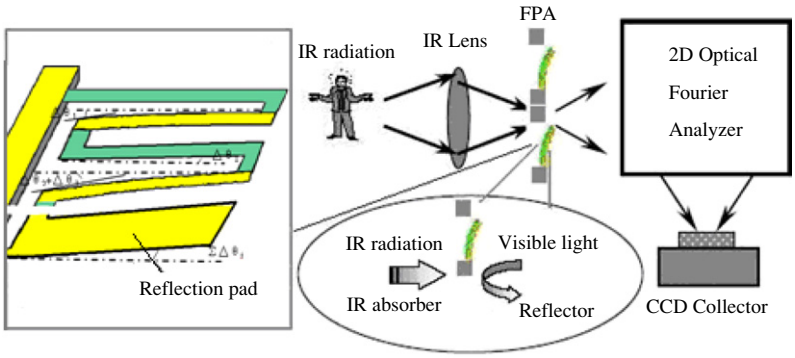

Figure 1. Schematic diagram of the uncooled optomechanical IR imaging system.

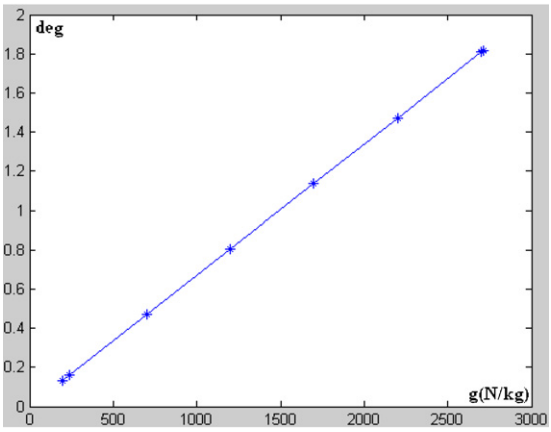

Figure 3. Relationship of inertial load and the maximum deformation angle of the IRFPA.

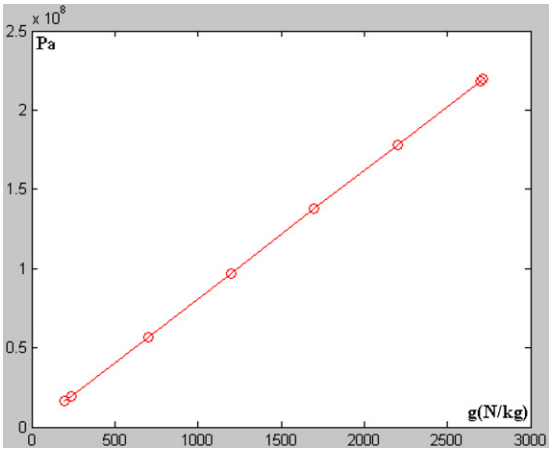

Figure 4. Relationship of inertial load and the maximum first-principles stress in the IRFPA.

the inertial load acceleration reaches 2715g, the maximum first-principles stress within the Au film is close to its yield strength (220 MPa [8]). Under this condition, the cantilever

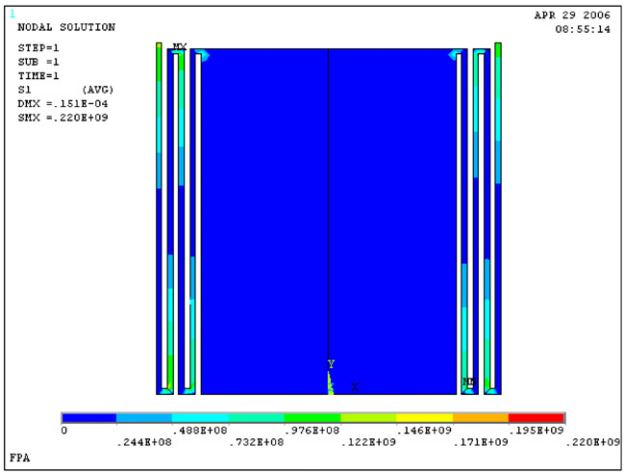

Figure 5. Distribution of the first-principles stress in the IRFPA under a load of 2715g.

structure will lose its linear response or even become plastic to the deformation induced by the inertial load, and the initial surface profile presents a conicoid characteristic. This is the critical point of failure imaging for the optomechanical readout. From figure 3, the maximum deformation angle induced by the inertial load of 2715g is about 1.8°. So according to equation (2), the linear range of optical detection should be within ±1.8°. The deflection response of the pixel's free end under the load of 2715g is shown in figure 6, from which the response time is about 1 ms. That means the deflection of each pixel under the critical inertial load reaches a steady value after about 1 ms. This determines that the frequency of the CCD collection frame should reach 1000 Hz. Thus a high quality optomechanical readout system is required.

3. Experiments

Not taking into account the quality requirement of the optomechanical readout system, the overloading ability of the IRFPA is 2715g, which is the simulated result from figure 4. It

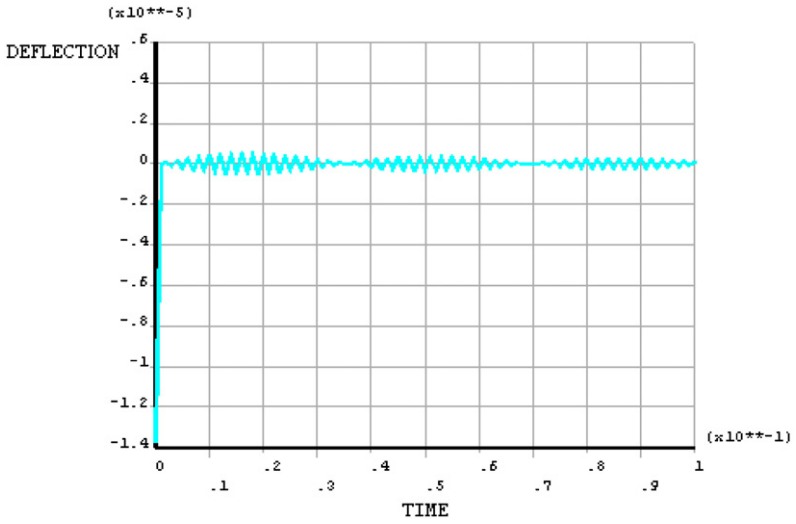

Figure 6. Deflection response of the pixel's free end under a load of 2715g.

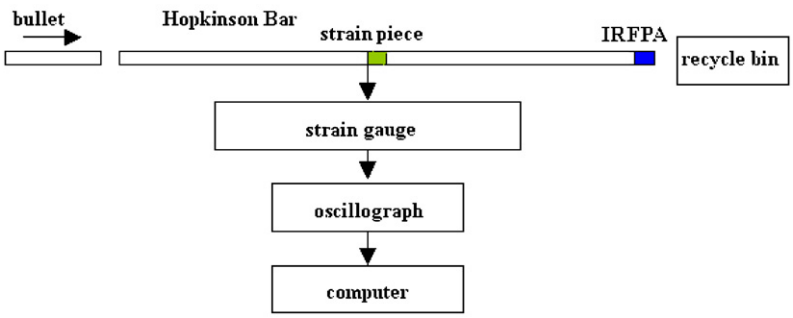

Figure 7. The setup of the shock experiment on the IRFPA chip.

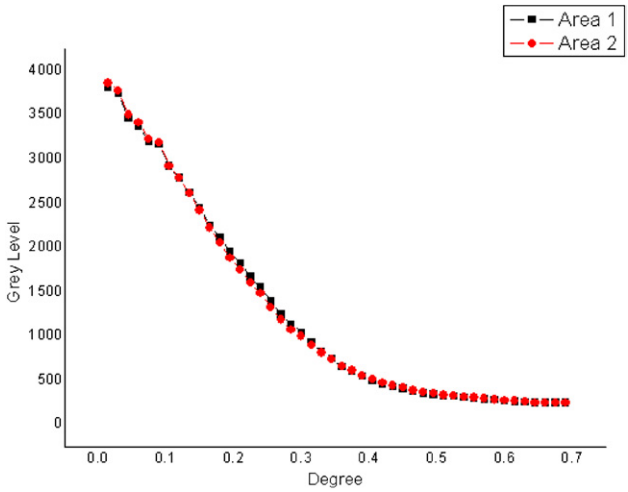

Figure 8. Graph of change in grey level versus change in FPA rotation angle.

could be validated through impact using a Hopkinson bar after the IRFPA is placed in vacuum (see figure 7) [9]. Because placing the IRFPA in vacuum is a problem that our team has not solved successfully, a validation of the failure analysis of the IRFPA presented in this paper under a high-g inertial load should be the target of future work after the placement in vacuum is successfully solved.

As analysed in section 2, if the uncooled optomechanical IR imaging system is to be used in a high-g environment ($2715g$), a high quality of optomechanical readout system is required. Our CCD collection frame frequency is only 30 Hz and the linear range of optical detection is within $\pm 0.3^\circ$ obtained in the experiment (see figure 8). These conditions can only ensure that the whole system undergoes an overloading of $448g$ as estimated by simulation.

4. Conclusion

Finite element simulation and the Hopkinson bar are methods for analysing the failure of an uncooled infrared focal plane array under a high-g inertial load. Regardless of the overloading ability of the optomechanical readout system, the simulated result is $2715g$. Validation of the failure analysis of IRFPA under a high-g inertial load is a target for future work after the placement in vacuum is successfully solved. Based on our optomechanical readout system, the CCD collection frame frequency and the linear range of the optical detection limit, the overloading ability of the whole system is $448g$. Although this capability could satisfy military applications at present, widespread application requires improvement of the quality of the optomechanical readout system. All our analysis is based on the common assumption that the FPA is perpendicular to the load acceleration; the result when the FPA is in the plane of load acceleration is a separate case not included in this paper.

Acknowledgment

This work was supported by the National Natural Science Foundation of China (no 60576053).

References

[1] Li C *et al* 2006 A novel uncooled substrate-free optical-readable infrared detector: design, fabrication and performance *Meas. Sci. Technol.* **17** 1981–6
[2] Ren L and Qu Y 2004 The application of millimeter wave technology and infrared technology in the martial field *Infrared Technol.* **26**
[3] Gurmpasla S D 2000 Recent development and applications of quantum well infrared photodetector focal plane arrays *Proc. SPIE* **4028** 262–75
[4] Laeau A G 2002 Tactical airborne reconnaissance goes dua1-band and beyond *Photonics Spectra* July 42–66
[5] Rockwell D L 2002 Recce pieces *J. Electron. Defense* June 45–50
[6] Shi S *et al* 2006 Design, simulation and validation of a novel uncooled infrared focal plane array *Sensors Actuators* A at press
[7] Zhao Y 2002 Optomechanical uncooled infrared imaging system *Dissertation* University of California, Berkeley
[8] Espinoza H D and Prorok B C 2003 Size effects on the mechanical behavior of gold thin films *J. Mater. Sci.* **38** 4125–8
[9] Huan Y *et al* 2003 Study of shock-resistibility of high-g microaccelerometer chip through impact using Hopkinson bar *Chin. J. Sensors Actuators* **16** 128–31